Journal of Power Sources 401 (2018) 55–64

Contents lists available at ScienceDirect

Journal of Power Sources

journal homepage: www.elsevier.com/locate/jpowsour

Structural engineering of S-doped Co/N/C mesoporous nanorods via the Ostwald ripening-assisted template method for oxygen reduction reaction and Li-ion batteries

Wanxin She, Juan Wang, Xiangyu Zhang, Mingchen Sun, Chuyi Xie, Junwu Xiao*, Shuai Wang**

Key Laboratory of Material Chemistry for Energy Conversion and Storage, Ministry of Education, Hubei Key Laboratory of Material Chemistry and Service Failure, Department of Chemistry and Chemical Engineering, Huazhong University of Science & Technology, Wuhan, PR China

HIGHLIGHTS

- A facile template method is reported to synthesize S-doped Co/N/C MNR.
- The MNR structure is controlled on the basis of the Ostwald ripening effect.
- Highly dispersed Co/N/C active sites are formed to inhibit the self-aggregation.
- Introducing the S doping in the Co/N/C structure enhances the intrinsic activity.
- It demonstrates excellent ORR activity and enhanced Li storage performance.

GRAPHICAL ABSTRACT

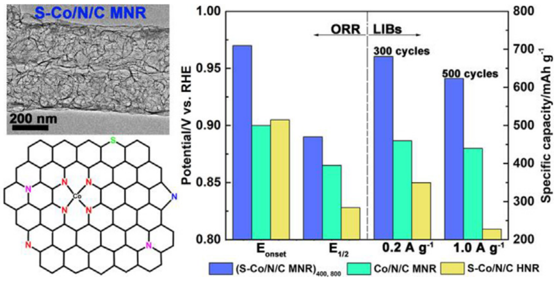

ARTICLE INFO

Keywords:
Structural control
Metal-nitrogen-carbon
C—S—C
Synergistic effect
Oxygen reduction reaction
Li-ion batteries

ABSTRACT

The long-debated intrinsic nature, less exposed active sites, as well as the tedious fabrication process of the metal-nitrogen-carbon structures severely impede the applications in the energy storage and conversion devices. Herein, we report a facile Ostwald ripening-assisted template method to controllably synthesize one-dimensional S-doped Co/N/C mesoporous nanorods as electrode materials for electrocatalytic oxygen reduction and Li-ions batteries. Introducing the S doping into the Co/N/C structure increases the intrinsic activity and electrochemically active surface area, and the structural characteristics (*e.g.*, the surface area, pore structure) of mesoporous nanorods are optimized on the basis of the Ostwald ripening effect for sufficiently exposing active centres and facilitating fast ion transport. Hence, it demonstrates efficient catalytic activity towards the oxygen reduction reaction in alkaline medium with the half-wave potential of 0.890 V vs. RHE, and even outerperforms the state-of-the-art Pt/C catalyst. In addition, as the anode material for Li-ion batteries, it also exhibits superior electrochemical performance with the specific capacity of 623.3 mAh g^{-1} after 500 cycles at 1.0 A g^{-1}.

1. Introduction

Rational design of carbon materials is critical for the development of cost-effective, high-performance energy conversion and storage devices, such as, fuel cells, metal-air batteries, Li-ion batteries (LIBs), etc. [1–3], and has recently attracted tremendous interest. There are two crucial factors to govern the electrochemical performances. One is the chemical environment, which influences the interactions between

---

* Corresponding author.
** Corresponding author.
E-mail addresses: chjwxiao@hust.edu.cn (J. Xiao), chmsamuel@hust.edu.cn (S. Wang).

https://doi.org/10.1016/j.jpowsour.2018.08.074
Received 1 June 2018; Received in revised form 21 August 2018; Accepted 24 August 2018

the electrode and electrolyte, and enhances the intrinsic nature of the electrochemical properties [4,5]. Theoretical and experimental studies have reported that nitrogen and transition-metal species are incorporated into carbon structure to construct efficient metal-nitrogen-carbon (M/N/C, M = Fe, Co, Mn, etc.) centres, resulting in significantly improving the electrochemical performance.

Another is the structural features and electric conductivity [6,7], which determine the accessible part of the electrolyte, and the mass and electron transport characteristics. The M/N/C structures are generally synthesized via the pyrolysis of metal-organic frameworks (MOFs) or the mixture of nitrogen-containing precursors and transition-metal species [7–9]. However, it frequently fails in controlling the pore structure and inhibiting the self-aggregation of transition-metal species during the pyrolysis process, leading to less exposed active centres and poor mass transport characteristics. On one hand, a large amount of zinc species (over three times than that of transition-metal species) are consumed for inhibiting the self-aggregation of transition-metal species via the carbothermal reduction reaction, resulting in forming highly dispersed M/N/C centres [10,11]. However, high pyrolysis temperature (> 800 °C) would decrease the N content and influence the electron and chemical environments of the M/N/C active sites, leading to deteriorating the intrinsic activity. On the other hand, the template casting method is proposed for constructing the hierarchical pore structure [12]. However, the pore size determined by the template structure is difficult to be tunable, and the strong corrosive agents (*e.g.*, HF, NaOH) are utilized during the tedious preparation process to restrict the exploration. Thus, to enhance the electrochemical performance, a rational design of the M/N/C materials with the sufficient active sites and high intrinsic activity, is a great challenge but desirable, and can be realized by fine-tuning the chemical components, surface area, as well as hierarchical pore structures. Moreover, the additional S doping in the M/N/C structures can induce more electroactive sites [13], and boost the intrinsic activity due to influencing the electron and spin densities around the M/N/C centres [14–19]. However, the S-doped M/N/C structures are rarely reported.

Herein, on the basis of the morphological features of one-dimensional structure with the facile formation of the conductive network and fast mass transfer ability [20], we propose an Ostwald ripening-assisted template method to successfully prepare S-doped Co/N/C mesoporous nanorods (S—Co/N/C MNR) with the controllable structure as electrode materials for electrocatalytic oxygen reduction reaction (ORR) and Li-ion batteries (LIBs). Combining the unique structural characteristics with high intrinsic activity, the resultants show superior ORR catalytic activity to commercial Pt/C catalyst, outstanding long-term durability, as well as good tolerance to methanol crossover effect, and also demonstrate the enhanced reversible capacity and cyclic performance for electrochemical Li storage.

2. Experimental

2.1. Preparation of Co/N/C and S-doped Co/N/C mesoporous nanorods

The synthetic procedures are described as follows: First of all, 1.8 g of $CoCl_2{\cdot}6H_2O$ and 1.2 g of urea are dissolved in 400 ml of deionized water. The solution is then transferred into a 500 ml Teflon-lined stainless-steel autoclave and heated at 100 °C for 12 h. The precipitates are washed by deionized water for several times and dried at 60 °C, and are then thermally decomposed at 300–450 °C under air atmosphere for 1 h with a heating rate of 2 °C min^{-1} to form black Co_3O_4 powder. Subsequently, 0.2 g of Co_3O_4 powder is dispersed in 100 mL of tris (hydroxymethyl)aminomethane (Tris, 10 mM) and dopamine hydrochloride (DA, 2 mg mL^{-1}) solution with continuous stirring for 24 h at room temperature to form the Co_3O_4/polydopamine (Co_3O_4/PDA). The Co_3O_4/PDA is then thermally treated at 550 °C for 1 h with a heating rate of 5 °C min^{-1} and Ar flow of 200 sccm to form the Co/carbon nanorods (Co/CNR). It's subsequently dispersed in HCl solution (2.0 M) for 1–5 h at 60 °C with vigorous stirring to remove the Co nanocrystals. The products are washed by deionized water till the pH is closed to 7, and dried by using the freeze-drying method. Finally, it's sulfurized at 700–1000 °C for 1 h with a heating rate of 5 °C min^{-1} and Ar flow of 80 sccm using thiourea as sulfur sources to form the S-doped Co/N/C mesoporous nanorods. It's symbolled as the $(S\text{—}Co/N/C\ MNR)_{x,\ y}$, where the alphabet “x” and “y” represent the thermal decomposition temperature (300, 350, 400, and 450) and sulfidation temperature (700, 800, 900, and 1000), respectively. By comparison, the Co/N/C mesoporous nanorods (Co/N/C MNR) are obtained as its pyrolyzed at 800 °C under Ar atmosphere (200 sccm) in the absence of thiourea.

2.2. Materials characterizations

The morphologies were examined by scanning electron microscopy (SEM) using Nova NanoSEM 450 at an accelerating voltage of 10 kV and transmission electron microscopy (TEM) on an FEI Tecnai G2 F20 microscope operating at 200 kV. Scanning transmission electron microscopy (STEM) and electron energy loss spectroscopy (EELS) mapping analysis were carried out on Titan G2 60–300 Probe Cs Corrector UHRSTEM. X-ray diffraction (XRD) was performed on a Philips PW-1830 X-ray diffractometer with Cu kα irradiation ($\lambda = 1.5406$ Å) with the step size of 0.05° and scan rate of 0.025° s^{-1}. X-ray photoelectron spectroscopy (XPS) was performed on a Perkin-Elmer model PHI 5600 XPS system with a resolution of 0.3–0.5 eV from a monochromated aluminum anode X-ray source with Kα radiation (1486.6 eV). Brunauer-Emmet-Teller (BET) surface area and Barrett-Joyner-Halenda (BJH) pore size distribution were analyzed from N_2 sorption isotherms at 77 K using a Micrometritics ASAP 2020 instrument. The Co contents were carried out on microwave plasma-atom emission spectrometer (MP-AES) (Agilent 4100, USA).

2.3. Electrocatalytic oxygen reduction reaction (ORR) measurements

It‘s carried out by using a potentiostat (IVIUM Vertex, Netherlands) and the rotating ring-disk electrode (RRDE-3A) system in a three-electrode configuration. The electrolyte is O_2-saturated 0.1 M KOH aqueous solution. The working electrode (WE) was prepared by dropping 5 μL of the dispersion, which was composed of 5.0 mg of the catalysts, 0.49 mL of N, N-Dimethylformamide (DMF) and 10 μL of Nafion solution (5 wt %), on a glassy carbon rotating disk electrode with 4 mm in diameter. The mass loading of the catalyst is ~0.4 mg cm^{-2}. For comparison, the state-of-the-art Pt/C electrode with the mass loading of ~0.4 mg cm^{-2} (0.08 mg_{Pt} cm^{-2}) was prepared via the same procedures using commercial Pt/C catalyst (Johnson Matthey, 20 wt%). Carbon rod and Hg/HgO (1.0 M KOH) electrodes were the counter electrode (CE) and reference electrode (RE), respectively. The electrode potential is converted relative to the reversible hydrogen electrode (RHE) potential using the following equation: $E_{RHE} = E_{(Hg/HgO)} + \varphi(Hg/HgO) + 0.0591{*}pH$ V.

Cycle voltammetry (CV) experiments were conducted at a scan rate of 10 mV s^{-1} in the potential range of 1.1–0.3 V. Linear sweep voltammograms (LSVs) were carried out from 1.1 to 0.3 V at a scan rate of 5 mV s^{-1} with varying rotating speed from 400 to 2400 rpm. Normalized current densities were given in terms of geometric area (mA cm^{-2}). Koutecky-Levich plots (J^{-1} vs. $\omega^{-1/2}$) were analyzed at the electrode potentials of 0.6–0.8 V, and the best-fit slopes were used for calculating the electron transfer number (n) on the basis of the Koutecky-Levich equation:

$$1/J = 1/J_k + 1/J_L = 1/J_k + 1/(B\omega^{1/2}) \qquad (1)$$

$$B = 0.62nFC_oD_o^{2/3}\nu^{-1/6} \qquad (2)$$

$$J_k = nFkC_o \qquad (3)$$

Where J is the measured current density, J_k and J_L are the kinetic- and